

A more consistent explanation of the strength of $\text{Al}_2\text{O}_3/\text{SiC}$ nanocomposite after grinding and annealing[☆]

C.C. Anya*

37 Beech Crescent, Kidlington, Oxford OX5 1DP UK

Received 27 May 1999; received in revised form 26 July 1999; accepted 25 August 1999

Abstract

In a recent paper it was proposed that the strengthening of 5 vol% SiC Al_2O_3 –SiC nanocomposite after grinding and annealing is attributable to flaw healing, in parallel with an oxidation reaction, which lead to a reduction in the density and size of flaws on annealing. Other authors have also favoured the flaw healing mechanism. However, the possibility that a mechanism based on dislocation activities might be mostly responsible has never been fully investigated. In this report the two mechanisms are investigated and it is demonstrated that the latter is more consistent with experimental observations. Possible sources of the ambiguity met in some of the explanations of the mechanisms behind the strengthening phenomenon are also identified. © 2000 Elsevier Science Ltd and Techna S.r.l. All rights reserved.

Keywords: B. Nanocomposite; C. Strength; Fracture toughness; Dislocations

1. Introduction

Various reasons have been advanced to explain the observed higher flexural strength of 5 vol% Al_2O_3 –SiC nanocomposite relative to monolithic alumina, particularly in the annealed state. Flaw healing mechanism was proposed by Wu et al. [1]. Zhao et al. [2] also favoured this mechanism, together with that based on compressive residual stress. However, Chou et al. [3] found that both the nanocomposite and alumina showed similar quantitative response to machining, and, therefore, concluded that the earlier proposed [2] residual stress mechanism is neither confirmed nor disputed. But it was implied [2] that stress relief during annealing (by bulk and grain boundary diffusion) facilitates surface flaw healing.

Dislocation activities have also been suggested [4] as another mechanism through which the strengthening occurs. Although dislocations are rarely present in alumina, it has been demonstrated that under certain stress

state they are generated in the monolith [5,6] and abundantly in Al_2O_3 –SiC_(P) nanocomposites [4,6–8]. Strengthening of metallic alloys through dislocation–dislocation and/or dislocation–particle interactions is well known. In comparison with metals, modern engineering ceramic materials do not yield much before failure. However, since some plastic yielding (dislocation generation) is observed during their deformation, any factor that constrains the limited yielding that takes place is most likely to raise their strength. Thus, the presence of dislocations, and their role in the alumina system, particularly in the annealed state where the conditions during annealing promote dislocation activities are worth investigating. Studies on the strengthening of the nanocomposites following annealing [1,2] never considered the possible role of dislocations in the phenomenon.

The potential of nanocomposite technology can only be fully utilised if the phenomena observed in the material are unambiguously explained and understood. The ambiguity, particularly in the annealed samples, derives from two possible sources. First, if the annealing studies use surface features to arrive at their conclusions, the samples being studied may be so degraded that they may no longer represent the original material for which the study is aimed at. Second, authors may be biased to

[☆] The results on which this report is based were obtained while the author was an employee of the Department of Materials, University of Oxford, Oxford OX1 3PH, UK.

* Tel.: +44-1865-841-974; fax: +44-1865-841-975.

E-mail address: c.anya@virgin.net (C.C. Anya).

impose an assumed principle, rather than exploring to find out the actual one behind the experimental observations. This report focuses on the flaw-healing and dislocation-based mechanisms for the strengthening and toughening phenomena experimentally observed in the material, and in relation to alumina. It also discusses the above mentioned sources through which erroneous representations of experimental observations could take place.

2. Experimental results

The results were obtained [6,9–11] on pressureless sintered materials, of which the 5 vol% SiC nanocomposite and the monolithic alumina discussed here sintered [11] to $\geq 99.8\%$ of their theoretical density (TD). It is important that for an objective comparison of the properties of these materials that their grain sizes and degree of densification are identical. The latter is particularly important for studies on surface properties, which depend on the elastic constants. For instance, the nanocomposite sintered to 98.2% TD was found [10] to have a value of Young's modulus (E) 4% less than that which sintered to 99.8% TD. It was also necessary to get rid of the reaction layer before the elastic constants were determined; otherwise the determinations no longer truly represent those of the material under study.

Examination [6] of the surfaces in plan (polished samples) and cross-section (fracture surfaces) under the scanning electron microscope (SEM) revealed maximum flaw sizes of about $3.8 \pm 0.5 \mu\text{m}$ for alumina and $3.5 \pm 0.5 \mu\text{m}$ for the nanocomposite. Hertzian indentation study of the two (polished samples) also revealed very similar sizes of about $5.2 \mu\text{m}$ for alumina and $4.5 \mu\text{m}$ for the nanocomposite. In ground state (14- μm diamond) the maximum flaw size for alumina is about $13 \mu\text{m}$ and $8 \mu\text{m}$ for the nanocomposite (Fig. 1). From this figure it is evident that by summing up the densities of each of the plotted small flaws ($\leq 5 \mu\text{m}$) the overall density of flaws (within this range) for the nanocomposite is only about double that in alumina. In Fig. 2 is a comparison of polished and ground samples of the nanocomposite. All the flaws in the polished state are in the small range ($\leq 5 \mu\text{m}$), and by a similar computation as above, their overall density in the polished state is more than 4 times that in the ground state.

Investigations [11] under the transmission electron microscope (TEM) revealed that in the nanocomposite there are sub-micron radial flaws, some as small as 150 nm. These sub-micron cracks develop from the thermal expansion coefficient mismatch between alumina and the SiC particles, which creates thermal stresses on cooling the samples (after sintering) from a certain temperature. The thermal stresses, in parallel with the creation of these radial sub-micron cracks, also lead to a generation of dislocations [6] (Fig. 3a), with a structure

different from that obtained on deforming the material (Fig. 3b).

3. Discussion

3.1. Toughness of alumina and 5 vol% SiC nanocomposite

Zhao et al. [2] argued that the toughening observed in the nanocomposite is derived exclusively from compressive stresses, hence the suggestion that the addition of SiC particles does not affect the intrinsic material

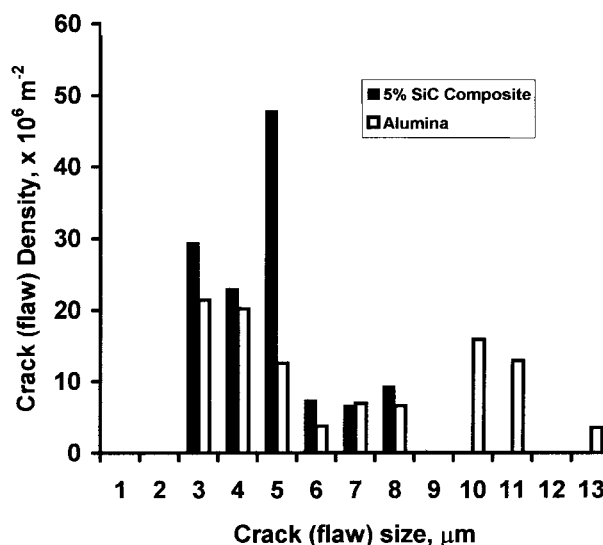


Fig. 1. Crack (flaw) density vs crack size for ground (14- μm diamond) for alumina and the nanocomposite. Note that the density of small flaws ($\leq 5 \mu\text{m}$) in the nanocomposite is only about double that in alumina.

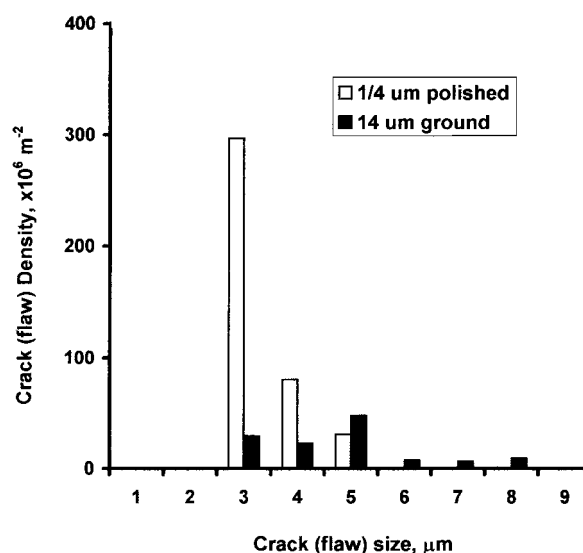


Fig. 2. Crack density vs crack size for polished and ground nano-composite. Note that the density of small flaws ($\leq 5 \mu\text{m}$) in the polished state is more than four-fold of that in the ground state.

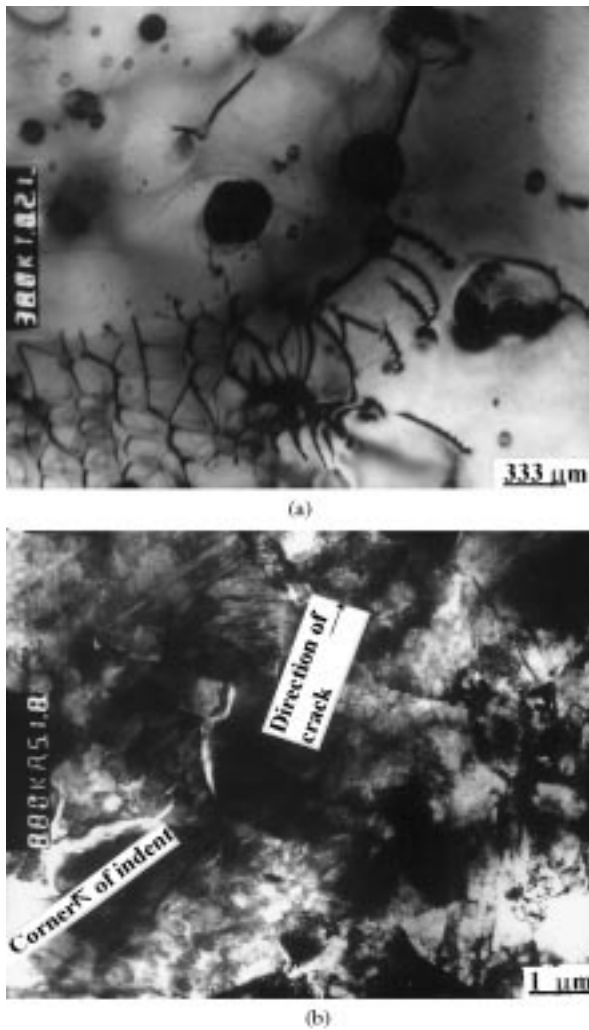


Fig. 3. Dislocation networks in 5 vol% SiC alumina/SiC nanocomposite: (a) sintered sample; (b) sintered and deformed by Vickers microindentation. Note the difference in structure.

toughness. However, Chou et al. [3] demonstrated that a similar magnitude of compressive stress is induced in alumina and the nanocomposite. So the higher toughening observed in the work of Zhao et al. [2] for hot-pressed nanocomposite is, after all, due to a combination of microstructural features induced by the addition of SiC particles — an effect that is intrinsic to the nature of the nanocomposite. Details of the various ways through which microstructural features combine to strengthen and toughen simultaneously can be found in other papers [6,11]. A typical example of toughening through crack bridging by particles is shown [11] in Fig. 4 — a bridge of only about 200 nm. Many such bridges along a crack path would dissipate its propagating energy. Note also the secondary crack on the particle (P), ‘sc’, which also would contribute to the dissipation.

Intrinsic toughness $K_{Ic(HERTZ)}$ of a material under a test is expressed [1,9] as a function of the minimum Hertzian indentation-cracking load, P_{min} , the elastic

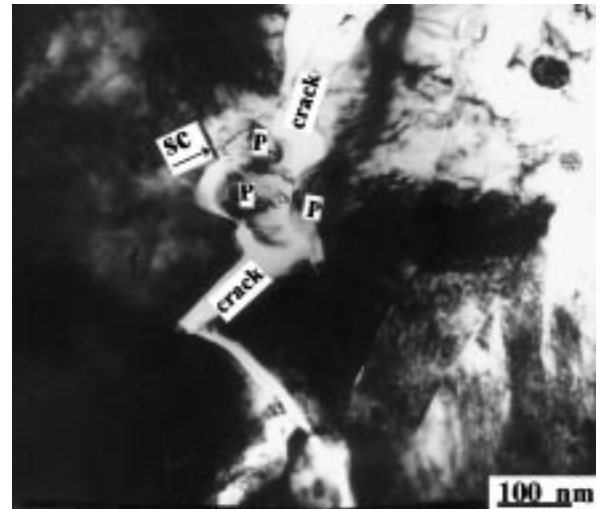


Fig. 4. A typical particle (P) bridging a primary crack propagating in 5 vol% SiC alumina/SiC nanocomposite. Note the secondary crack, ‘sc’, on a SiC particle. Note also the ‘new’ dislocations as in Fig. 3b.

properties, E^* and C (a constant that depends on Poisson’s ratio, ν), and the radius of the blunt ball indenter, R , according to the equation:

$$K_{Ic(HERTZ)} = \sqrt{\frac{E^* P_{min}}{CR}} \quad (1)$$

and E^* is defined [12] as:

$$E^* = \frac{E}{2(1 - \nu^2)} \quad (2)$$

Eq. (2) holds only when the indenter and substrate materials are elastically similar. From Eq. (1) it is evident that the intrinsic toughness of a material will change with any modification to its elastic constants, as well as P_{min} .

It is worth defining the relationship between $K_{Ic(HERTZ)}$ and K_{Ic} . The former may determine only at what load a crack is initiated from an existing flaw. Beyond this stage the K_{Ic} determines to what extent the initiated crack would grow before the material fails. In other words, the critical stress intensity factor for K_{Ic} is much higher than that for $K_{Ic(HERTZ)}$. Thus K_{Ic} is made up of the two components; the intrinsic, $K_{Ic(HERTZ)}$, and another accruing from the interaction of the growing crack with internal microstructural and fractographic features in the material. Whereas $K_{Ic(HERTZ)}$ is determined using the elastic constants obtained on the surface of the material, K_{Ic} is a bulk material property, and, therefore, is of more practical relevance. Porosity can affect both $K_{Ic(HERTZ)}$ and K_{Ic} . The effect on the former is mostly through the elastic constants. Providing porosity is about the same for both alumina and the nanocomposite the latter has always been shown [2,4,13,14] to be of a higher K_{Ic} value.

Wu et al. [1] suggested that the intrinsic toughness of alumina and the nanocomposite are very similar, and cited some other reports [2,13,15–17] in support of this. However, in the reports [13,16,17] the topic of intrinsic toughness was not studied at all, and the nanocomposite was observed to show a higher value of K_{Ic} by up to 6%. Although Zhao et al. [2] had argued that the addition of SiC particles did not affect the intrinsic toughness of the nanocomposite, their work does not in any way suggest that its value is similar to that of alumina. This is particularly so for the hot-pressed materials — similar to the state of the samples used by Wu et al. [1] — where the TD, which could affect toughness, is the same for both materials. The argument that in stable brittle composite materials the intrinsic toughness could be that of the predominant matrix might be used to justify the suggestion by Wu et al. [1] that the intrinsic toughness of alumina and the nanocomposite to be similar. However, intrinsic toughness, as defined in the present and other [1,9] reports is affected by the modification of elastic constants [Eqs. (1) and (2)]. Therefore, so long as the added secondary phase induces this modification, as has been demonstrated [9], the intrinsic toughness of the two is most unlikely to be similar. The few [9,15] available reports on the Hertzian indentation study of Al_2O_3 –SiC nanocomposite clearly demonstrate that $K_{Ic(HERTZ)}$ of the nanocomposite is higher than that of alumina. In both studies $K_{Ic(HERTZ)}$ values for 5 vol% SiC nanocomposite were found to be greater than that of alumina by 3–20%, depending on the type of SiC used [15] and about [9] 28%.

3.1.1. Assessment of minimum Hertzian indentation cracking load, P_{min} and its relationship with intrinsic toughness ($K_{Ic(HERTZ)}$)

P_{min} is associated [1] with the residual stress on the surface of the material under Hertzian indentation, and its lowest value is obtained on a surface that is devoid of residual stress. This condition is best met in polished and annealed samples. During annealing residual stress is relieved [1,3] at a faster rate in alumina in comparison

with the nanocomposite. However, in their [1] work, for the ground-annealed specimens, P_{min} was not determined for alumina due to its poor surface, but they found it to decrease from about 1400 to 500 N for the nanocomposite. So they concluded that the intrinsic toughness of alumina and the nanocomposite are very similar, even though they did not measure P_{min} for ground-annealed alumina. Depending on the severity of the grinding process, some residual stress (that determines P_{min}) is still retained in alumina after annealing, though to a lesser extent than in the composite [3].

The conclusion that the intrinsic toughness of alumina and the nanocomposite are very similar [1] is over simplistic. First, because residual stress on which P_{min} (that partly determines the intrinsic toughness) depends also diminishes in alumina, and therefore, in the same annealed state (as the nanocomposite) its P_{min} should be lower than that in ground state. By how much lower is the question that should have been answered, had they measured it. Second, from Eq. (1) it can be seen that intrinsic toughness, $K_{Ic(HERTZ)}$ depends on three variables and the radius of the ball indenter, R . For instance, a mere increase of Poisson's ratio from 0.24 to 0.25 increases [12] the constant, C , from 2790 to 3131 — an increase of 12.2%. The next logical question would be which of the two variables, E and P_{min} affects the intrinsic toughness more. In Table 1 is shown the effect of changes in these two variables on intrinsic toughness. In this table the first row is an experimental result [9], while the second is a hypothetical extrapolation from the first. It can be seen that whereas about 5% change in toughness is achieved by a 10% change in P_{min} , only about 2% change in E is required. Since E of the nanocomposite is always higher than that of alumina [1,9], and with such a strong dependence of intrinsic toughness on E , the value of the former is most likely to be higher in nanocomposite than in alumina. Further, since the more controlling factor — change in elastic constants — is present, the contribution of P_{min} to intrinsic toughness becomes secondary. However, a change in elastic properties (as was present in the work

Table 1

Effect of a change in Young's modulus, E , and minimum Hertzian cracking load, P_{min} on intrinsic toughness, $K_{Ic(HERTZ)}$ of 5 vol% SiC alumina/SiC nanocomposite

E (GPa)	P_{min} (N) Surface finish		$K_{Ic(HERTZ)}$ (MPa m ^{1/2})		ΔE (%)	ΔP_{min} (%) ^a	$\Delta K_{Ic(HERTZ)}$ (%)
	Polished	Ground ^b	Polished	Ground			
399.5 ± 4 ^c	465 ± 11	511 ± 14	3.56 ± 0.1	3.73 ± 0.1	0	9.9	4.8
407.5 ^d	465	511	3.59	3.77	2	9.9	5

^a Relative to the value for the polished sample.

^b 14-μm diamond.

^c Experimental result (Ref. [9]).

^d Calculated for an increase of 2% in E , with P_{min} kept constant.

of Wu et al. [1]) will automatically affect the whole components of Eq. (1) (apart from R). Therefore, a relationship between the intrinsic toughness of the material and only a minor component such as P_{\min} is unreliable.

3.1.2. Chemical integrity of the annealed surface

Wu et al. [1] indicated that the surface stiffness of the nanocomposite after annealing changed due to the formation of amorphous mullite of a lower elastic modulus (more on the possibility of formation of mullite in Section 3.2.1). Although they did not indicate to what thickness this layer was formed, it is clear that the annealed surface of the material they studied is at the best that of a composite of the formed layer/nanocomposite, and at the worst that of just the layer. Even if no layer was formed, that is the SiC particles on the surface simply oxidised, again the same problem of the surface under study no longer being typically that of the nanocomposite remains. However, the elastic properties associated with P_{\min} (implicitly the intrinsic toughness, according to Wu et al. [1]) should be for the surface of the material under study.

3.2. Strengthening mechanisms

Standard fracture mechanics of a brittle material [Eq. (3)] suggests that for a given critical flaw size an increase in fracture toughness as argued in this work, and shown in other reports [2,4] to obtain in the nanocomposites, is responsible for the increase in strength.

$$\sigma_f = \frac{K_{Ic}}{Y(C)^{1/2}} \quad (3)$$

where σ_f is the fracture stress and K_{Ic} is the fracture toughness of the material. Y is a constant [6] and C is the critical flaw size.

However, with modern engineering ceramics this suggestion is hardly experimentally observed; for instance, it has been demonstrated [2] that though the strength of annealed 5 vol% SiC nanocomposite increased, its fracture toughness was reduced.

3.2.1. Flaw healing mechanism

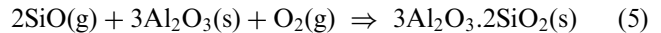
3.2.1.1. Blunting of strength-limiting surface flaws by oxide layers. Nature of the layers. This section discusses the ambiguity derivable from assuming that a popular principle applies in an experiment, without observing that the features that support the principle are present.

Eq. (3) suggests that for a given value of fracture toughness reducing the critical surface flaw size would increase strength. On this basis surface treatments aimed at blunting strength-limiting surface flaws have been carried out. One such example by Kim et al. [18] involves the formation of oxide (mullite) surface layers

on alumina. Using a bed of SiC platelets as a constant supply source, Kim et al. [18] produced at 1400°C some SiO₂ “smoke”, which in turn reacted with alumina to form mullite on its surface according to the equation:



They confirmed the formation of mullite by X-ray Diffraction (XRD) patterns. Wu et al. [1] used the result of Kim et al. [18] to support their suggestion of forming mullite according to the equation:



But the two situations are not the same. In Eq. (4) the source of SiC from which the SiO₂ “smoke” is formed is plentiful — a separate bed of loose SiC platelets, with a continuous supply of humid H₂ gas. However, in the case of Eq. (5) the SiC particles are bound with matrix alumina.

Analytically, Wu et al. [1] indicated that X-ray analysis of the *amorphous* mullite confirmed the presence of Si. X-ray diffraction method neither shows the elements in a phase nor peaks (from which a phase could be identified) for amorphous phases. By what ever means they observed Si, its source could be from SiC and/or secondary silica-rich phases of the nanocomposite.

Balancing a chemical equation does not necessarily mean that the reaction so favoured occurs. The thermodynamic criterion [19] also has to be met. Hence for a reaction to occur,

$$\text{Log}K = \sum v_i \text{Log}K_f(i) \quad (6)$$

where K is the reaction constant, v is the molar volume of specie, “ i ”, which is considered to be negative for reactants and positive for products. K_f is the equilibrium constant of pure specie, “ i ”. The reaction also has to satisfy the Gibbs energy requirement:

$$-\text{Ln}KRT = \Delta G_F(T) \quad (7)$$

where $\Delta G_F(T)$ is the sum of the individual standard Gibbs energy of pure species, “ i ” at the absolute reaction temperature, T (respecting the signs for reactants and products). R is gas constant, which is 8.31441 JK^{−1}mol^{−1}. Thermodynamic data [19] of reactions proposed by Eqs. (4) [18] (at 1673 K) and (5) [1] (at 1523 K), and at temperatures as close as possible to those where equilibrium could be attained (1680 K for Eq. (4) and 1500 K for Eq. (5)) were obtained (Table 2). Using the data the values of the reaction constant, K in Eq. (6) for each of the reactions proposed at the temperatures used by the authors [1,18] and those at which equilibrium could be attained, are calculated. The left and right members of Eq. (7) can also be calculated with the thermodynamic data. These are shown in Table 3.

From Table 3 it is evident that equilibrium can be attained for the system proposed by Kim et al. [18] at 1680 K — a temperature well within an acceptable range of fluctuation for a furnace set to attain 1673 K. On the other hand, the reaction proposed by Wu et al. [1] never attains equilibrium. This indicates that the reaction proposed by them is not possible under the conditions they stated.

With a sufficient partial pressure of SiO Kim et al. [18] observed mullite by XRD in a sample heated just for 1 h. But when a 5 vol% SiC alumina/SiC nanocomposite was thermally etched [10] for 1.5 h at 1400°C in argon, though the SiC particles on the surface of the sample were oxidised, no mullite was detected by XRD and EDAX analyses on the sample. This is because the oxidation of the surface particles is not enough to generate the necessary partial pressure of SiO required to form mullite. Once the SiC particles on the surface have been oxidised the alumina matrix protects those below. A similar suggestion was also made [20] about the protection of SiC whiskers in alumina/SiC composite.

3.2.1.2. Density of healable flaws. Wu et al. [1] favoured a flaw-healing mechanism based on the principle that relative to alumina, a greater density of more healable small cracks are found on the nanocomposite surface. Following this principle, if small cracks (of the same size as found on the nanocomposite) are present on alumina surface (albeit at a reduced density) (Fig. 1) some healing should also take place in the latter. This should lead to a strengthening effect in alumina proportional to the density of healable cracks in it, but on the contrary, a

Table 2

Thermodynamic data of substances at temperatures^a related to the work in refs. 1 and 18

Substance	Temperature (K)	ΔG_f° (kJ mol ⁻¹)	Log K_f
α -Al ₂ O ₃	1500	-1196.322	41.660
	1523	-1188.796	40.815
	1673	-1139.782	35.625
	1680	-1137.498	35.398
Mullite	1500	-4899.653	170.621
	1523	-4899.989	167.197
	1673	-4675.404	146.131
	1680	-4666.308	145.211
SiO ₂	1500	-644.487	22.443
	1523	-640.59	21.993
	1673	-614.885	19.218
	1680	-613.671	19.097
SiO	1500	-227.551	7.924
	1523	-229.350	7.869
	1673	-240.710	7.518
	1680	-241.222	7.502

^a These temperatures are those used by the authors [1,18] and those closest to where equilibrium could be attained (see text).

Table 3

Satisfaction of Gibbs energy criterion [Eq. (7)] for the relative systems (proposed in Refs. [1] and [18]) for forming mullite

K	T (K)	$\Delta G_F(T)$ (Jmol ⁻¹)	LnKRT	Reference
6.21×10^{29}	1500	-855 585	855 564	[1]
1.03×10^{29}	1523	-844 901	845 923	
6.607	1673	-26 288	26 264	[18]
6.653	1680	-26 472	26 471	

reduction in strength is observed after alumina is annealed (Table 4).

Wu et al. [1] explained the lack of response from alumina on the basis of its cracks' depth being much larger than the extent of any machining-induced compression. Assuming this is the case, those cracks that are of the same depth as those found in the nanocomposite should lead to strengthening as they do in the latter, but they do not. Similarly, in Fig. 2 it is evident that relative to a ground, a polished nanocomposite has more than 4 times the density of small flaws. Yet it can be seen in Table 4 that annealed (10 h) ground-polished nanocomposite (which should have more healable flaws) has less strength than the ground one.

In unannealed condition, higher strengths are obtained (for both alumina and the nanocomposite) in polished samples, because they contain critical flaws of sizes smaller than those found in the ground samples. As has been highlighted [6], flaw size controls strengthening phenomena only in the absence of other over-riding mechanisms. The critical flaws of smaller sizes in the annealed condition did not lead to an increase in strength in both materials studied by Wu et al. [1]. For the nanocomposite, comparison is made for samples subjected to the same duration (10 h) of treatment (Table 3). This ensures that only the effect of flaw healing is considered. It is evident that the flaw-healing mechanism does not satisfactorily explain the phenomenon observed. Therefore, there must be another mechanism that over-rides it.

3.2.2. Dislocation-based mechanism. Blunting of crack tip

A dislocation-based concept could explain why the role of flaw-size is relegated as a strength-controlling factor in annealed samples.

After sintering, alumina shows virtually no dislocation network. However, the nanocomposite exhibits an appreciable dislocation density (Fig. 3a [6]), generated from the cooling stage of the sintering process. A TEM study of the plastic zones formed by Vickers microindentation (using a force of 2 N, which poses a stress-state similar to that met in machined samples) on alumina and the nanocomposite showed that, relative to the latter, alumina acquires a dislocation network of a very low density.

In the nanocomposite, the creation of more dislocations (from the microindentation) and the pre-existing ones lead to a very high density of dislocations relative

to alumina. The pre-existing dislocations (Fig. 3a), at room temperature tests are immobile. However, possible reactions between themselves and with the particles at the annealing stage could contribute to strengthening at room temperature. Reactions between dislocations are known [21] to generate immobile dislocations, which usually are barriers to other moving dislocations. The movement of the newly created dislocations at the room temperature test (Fig. 3b), is, therefore, restrained, and they blunt the crack tips. These activities, together with other fractographic features that develop within the nanocomposite sample at room temperature deformations [6], contribute to an increase in both strength and toughness. It was also demonstrated [11] that the sub-micron cracks induced by the particle addition blunt crack tips.

There might, therefore, be a threshold of dislocation density above which dislocation activities of the sort described above take hold. Below the threshold the activities are virtually absent, and only a relaxation of the stress that produced the few dislocations is achieved. Support for this hypothesis can be found in the fact that Fang et al. [7] observed that in annealed samples alumina has dislocation-free sub-grains, while dislocation entanglement remains in the nanocomposite. This finding might also explain the fact in Table 3 that annealed alumina has strengths lower than that of the polished unannealed samples.

Most of the reports on alumina/SiC nanocomposites consider only 5 vol% SiC composition. However, it has been demonstrated [4,16] that in terms of toughness the optimal addition of SiC particles, without much reduction of strength, seems to be beyond 5 vol%. Compositions with more than 5 vol% SiC particles have also been shown [22] to have a remarkable wear resistance. Since one of the main technical problems with alumina is its relatively poor thermal shock resistance, future work on this system could concentrate more on compositions with more than 5 vol% SiC, with a view to tapping the potential higher toughness. This will also offer the opportunity to investigate further the dislocation-based mechanism proposed in this report.

Generally, discontinuities in a body lead to a non-uniform stress distribution when an external load is applied. Positions occupied by a secondary phase in a composite could be viewed as discontinuities and, therefore, are likely to produce a similar effect.

The stress is usually concentrated around the discontinuities, and the external load could be thermal and/or mechanical. Very high values of stress concentration lead [6,11] to micro-crack formation and dislocation generation. The magnitude of the stress concentration depends on factors such as the relative compliance and coefficient of thermal expansion [CTE (α)] of the materials forming the composite. Irrespective of the source of the external load (mechanical and/or thermal), the effect of the latter seems to yield far more dislocations. This is because despite the small difference between the elastic moduli of alumina and SiC (with a ratio [10] of about 1:1.2), but a larger difference in CTE (with a ratio [11,23] of about 1:2) the composite generates quite a relatively high density of dislocations. However, a composite of alumina/TiN (with a ratio of their moduli of about 1:1.5, and of CTE of about [23] 1:1.06) shows [8] a very low density of dislocations after sintering, in comparison with that of alumina/SiC_(p). Therefore, it would seem that the difference in CTE between the secondary phase and alumina should be quite substantial to generate enough dislocations that would contribute to the strengthening and toughening of the composite. Another factor that would be worth considering is the ratio of the interfacial (matrix/particle) energy to that of the grain boundary (matrix). This has been argued [23] to affect interfacial fracture energy, which in turn controls strengthening. A very high interfacial energy could lead to the interface acting as dislocation sources. This suggestion is supported by experimental observations such as evident in Fig. 3a, where dislocations can be seen moving away from the particles.

Higher contents of SiC particles would lead to more areas with higher interfacial energy, and being subjected to stress concentrations resulting from the difference in CTE, both conditions leading to more dislocations to be generated for a given area.

Table 4
Flexural bend strengths achieved [1] for alumina and 5 vol% SiC nanocomposite, with different surface conditions and treatments

Material	Surface condition	Treatment	Strength (MPa)
Alumina	Ground	Unannealed	295 ± 20
	Ground + polished	Unannealed	430 ± 25
	Ground	Annealed, 2 h	280 ± 15
	Ground	Annealed, 10 h	250 ± 8
Nanocomposite	Ground	Unannealed	395 ± 120
	Ground + polished	Unannealed	540 ± 60
	Ground	Annealed, 2 h	615 ± 65
	Ground	Annealed, 10 h	680 ± 50
	Ground + polished	Annealed, 10 h	615 ± 65

4. Conclusions

A hypothesis on dislocation-based mechanism that is more consistent than that of flaw-healing is presented as a more probable cause for the strengthening, and its absence respectively in machined and annealed 5 vol% alumina/SiC nanocomposite and alumina.

The intrinsic and overall fracture toughness of the nanocomposite are higher than those of alumina. Several works cited by Wu et al. [1] to support their suggestion that the intrinsic toughness of alumina and the nanocomposite are similar never engaged in such a study.

It is analytically argued that the suggestion by Wu et al. [1] about the formation of mullite on the surface of annealed nanocomposite is inconsistent. It is also the case that such a reactive system is not supported thermodynamically under the conditions their work was carried out.

Explanations of the remarkable behaviour of alumina/SiC nanocomposites consistent with experimental observations require looking beyond standard (linear elastic) fracture mechanics of brittle materials.

Acknowledgement

The project from which the results presented here were obtained was funded by EPSRC, UK.

References

- [1] H.Z. Wu, C.W. Lawrence, S.G. Roberts, B. Derby, *Acta Mater.* 46 (1998) 3839–3848.
- [2] J. Zhao, L.C. Stearns, M.P. Harmer, H.M. Chan, G.A. Miller, R.F. Cook, *J. Am. Ceram. Soc.* 76 (1993) 503–510.
- [3] I.A. Chou, H.M. Chan, M.P. Harmer, *J. Am. Ceram. Soc.* 79 (1996) 2403–2409.
- [4] K. Niihara, *J. Ceram. Soc. Jpn* 99 (1991) 974–982.
- [5] B.J. Hockey, *J. Am. Ceram. Soc.* 54 (1971) 223–231.
- [6] C.C. Anya, *J. Mater. Sci.* 33 (1998) 977–984.
- [7] J. Fang, H.M. Chan, M.P. Harmer, *Mater. Sci. Eng. A* 195 (1995) 163–167.
- [8] S. Jiao, C.E. Borsa, C.N. Walker, *Silicates Industriels* 60 (1995) 211–214.
- [9] C.C. Anya, S.G. Roberts, *J. Eur. Ceram. Soc.* 16 (1996) 1107–1114.
- [10] C.C. Anya, S.G. Roberts, *J. Eur. Ceram. Soc.* 17 (1997) 565–573.
- [11] C.C. Anya, *J. Mater. Sci. Lett.* 16 (1997) 1300–1301.
- [12] P.D. Warren, *J. Eur. Ceram. Soc.* 15 (1995) 201–207.
- [13] R.W. Davidge, R.J. Brook, F. Cambier, M. Poorteman, A. O'Sullivan, D. O'Sullivan, S. Hampshire, T. Kennedy, *Br. Ceram. Trans.* 96 (1997) 121–127.
- [14] T. Ohji, A. Hirano, A. Nakahira, K. Niihara, *J. Am. Ceram. Soc.* 79 (1996) 33–40.
- [15] L.M. Carroll, M. Sternitzke, B. Derby, *Acta. Mater.* 44 (1996) 4543–4552.
- [16] C.E. Borsa, S. Jiao, R.I. Todd, R.J. Brook, *J. Microsc.* 177 (1994) 305–312.
- [17] L.C. Stearns, J. Zhao, M.P. Harmer, *J. Eur. Ceram. Soc.* 10 (1992) 473–477.
- [18] H.E. Kim, A.J. Moorhead, S.K. Kim, *J. Am. Ceram. Soc.* 80 (1997) 1877–1880.
- [19] I. Barin, *Thermochemical Data of Pure Substances*, 3rd ed., VCH Weinheim, Germany, 1995.
- [20] S.M. Smith, R.O. Scattergood, J.P. Singh, K. Karasek, *J. Am. Ceram. Soc.* 72 (1989) 1252–1255.
- [21] J. Weertman, J.R. Weertman, *Elementary Dislocation Theory*, Macmillan Publications, New York, 1964, p. 93.
- [22] C.C. Anya, *Ceram. Int.* 24 (1998) 533–542.
- [23] S. Jiao, M.L. Jenkins, R.W. Davidge, *Acta Mater.* 45 (1997) 149–156.